

CHSH inequality violation

Lucia Depaoli
lucia.depaoli.1@studenti.unipd.it
n° matricola: 2016960

August 30, 2022

Abstract

CHSH inequality violation project for Quantum Information and Computing course at University of Padova.

1 Introduction

1.1 Aim of experiment

In this experiment we want to violate the CHSH inequality in order to provide a proof of Bell's theorem. The form of CHSH inequality is the following:

$$|S| \leq 2 \quad (1.1)$$

Where:

$$S = E(\alpha, \beta) + E(\alpha, \beta') + E(\alpha', \beta) - E(\alpha', \beta') \quad (1.2)$$

The terms $E(\alpha, \beta)$ are the quantum correlations of particle pairs, defined to be the expectation values of the product of the outcomes of the experiment. α and β are the set of chosen angles. Each terms is calculated as:

$$E(\alpha, \beta) = \frac{N_{++} + N_{--} - N_{+-} - N_{-+}}{N_{++} + N_{--} + N_{+-} + N_{-+}} \quad (1.3)$$

The N_{ii} terms are the number of coincidences detected in the experiment and the denominator is a normalization factor.

Basically, pairs of photons are sent in different directions, towards a polarizer. After, two detectors are placed, one at the exit of the transmitted path and one and the exit of the reflected path. If the photon is detected in the transmitted detector, the output is $+$, otherwise it is $-$. The polarizers angles can be changed. If $E = 0$, then there is no correlation between the two photons, if $E = 1$ means that a correlation is present, whereas $E = -1$ means that an anti-correlation is present.

If the inequality in Eq.1.1 is violated, any local hidden theory is proven to incompatible for quantum mechanics.

1.2 Tools

The following list explain the tools we used in order to perform the experiment.

Spontaneous Parametric Down Conversion (SPDC) Type I: is a non-linear crystal used to generate entanglement. The functioning is shown in Fig.1. For the Type I SPDC we have the following two possible situations:

$$|H\rangle_p \rightarrow |VV\rangle_{is} \quad (1.4)$$

$$|V\rangle_p \rightarrow |HH\rangle_{is} \quad (1.5)$$

Where e means the extraordinary polarization, while o the ordinary polarization. It is possible to change the angle of the crystal in order to change the amplitude of the output cone. The entanglement

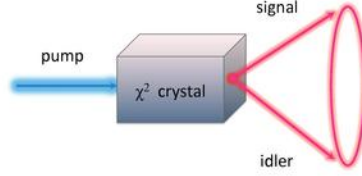


Figure 1: Functioning of Type I SPDC. The input photon p (pump) is separated into 2 output photons: i and s (idler and signal), which have the same polarization but orthogonal to the one of the input beam.

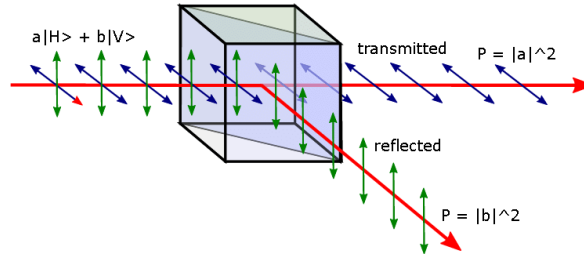


Figure 2: Input and output of a PBS. Usually, two detectors are placed at the output of the light beams.

can be created by sending a superposition of H and V through 2 SPDC crystal with perpendicular axis:

$$\frac{1}{\sqrt{2}}(|H\rangle_p + |V\rangle_p) \rightarrow \frac{1}{\sqrt{2}}(|VV\rangle_{is} + |HH\rangle_{is}) \quad (1.6)$$

Polarizing Beam Splitter (PBS): it is used in order to separate the two components of a light beam. The horizontal polarization is transmitted, whereas the vertical polarization is reflected, as shown in Fig.2.

Half Waveplate (HWP): it can be used to change the polarization of the light. It is possible to rotate the HWP. In this case, the rotation matrix that gives the output is:

$$M_\phi^{HWP} = \begin{pmatrix} \cos(2\phi) & \sin(2\phi) \\ \sin(2\phi) & -\cos(2\phi) \end{pmatrix} \quad (1.7)$$

In our case, we have the following conversion:

- $\phi = 0$: $|H\rangle \rightarrow |H\rangle$, $|V\rangle \rightarrow |V\rangle$
- $\phi = 45$: $|H\rangle \rightarrow |V\rangle$, $|V\rangle \rightarrow |H\rangle$
- $\phi = -22.5$: $|H\rangle \rightarrow |A\rangle$, $|V\rangle \rightarrow -|D\rangle$
- $\phi = 22.5$: $|H\rangle \rightarrow |D\rangle$, $|V\rangle \rightarrow |A\rangle$

By putting a HWP before a PBS, we can change the measurement basis.

1.3 Setup of the experiment

The setup of the experiment is shown in Fig.3. Photons are emitted from a laser with frequency 405 nm. The light beam pass through a lens that focus the light, and then it is reflected by 2 mirrors. At this point, a HWP is used to produce a light beam with Horizontal (H) polarization. After, the light pass through two Type I SPDC in order to create entanglement, and then it pass throughout a series

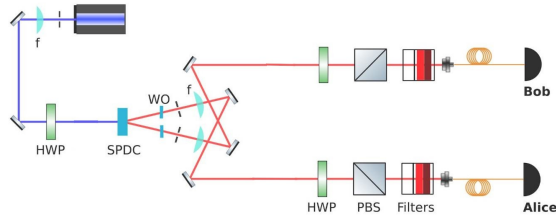


Figure 3: Laboratory setup.

α	β
0°	-22.5°
0°	22.5°
45°	-22.5°
45°	22.5°

Table 1: Set of different angles configuration.

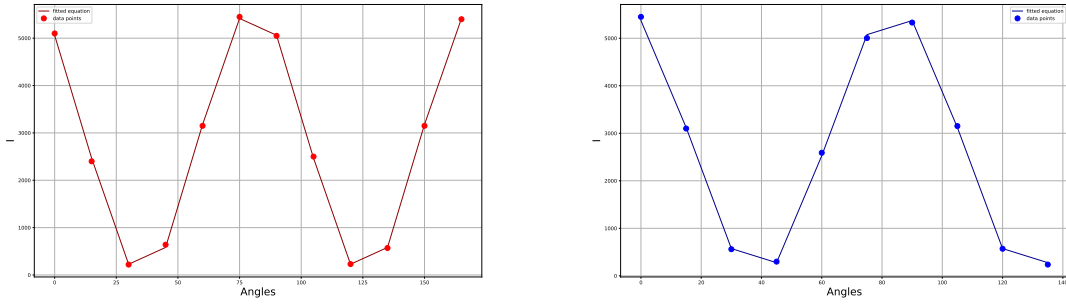


Figure 4: Calibration of the HWPs. On the left, the calibration for A , on the right the one for B .

of collider, because photons have to be indistinguishable each others. The entangled photons follow now two equal and parallel paths made up by a HWP (that can be rotated in order to change the basis), a PBS, some filters and a photon detector.

Given the rotational angles of the two parallel HWP, we have 4 different experiment configuration, shown in Tab.1, and 4 different measurement for each configuration (+ and – for A and the same for B), leading to a total of 16 different measurement.

Each measurement is recorded on a text file made up by 2 columns. The first one is the time of the recording (in bins of 81 ps) and the second is the channel in which the photon is detected (1 for A and 4 for B). Since each file records different time interval, they are cropped in measure of the one which have the smallest amount of data time recorded.

2 Waveplate calibration

We have to calibrate the HWPs in order to find the rotational angles for which the plates have the optical axis in vertical direction. Two sets of measurement are done, one for HWP_A and one for HWP_B , recording the different angles and the number of coincidences detected. At this point, Malus' Law (Eq.2.1) is fitted using SCIPY.OPTIMIZE.CURVE.FIT function.

$$I = I_0 \cos(\theta - \theta_0)^2 + offset \quad (2.1)$$

We are interested only in the θ_0 parameter. From the fit we get: $\theta_A = -18.62^\circ$ and $\theta_B = -11.94^\circ$. In Fig.4 are shown the results of this operation. At this point, the set of rotational angles are fixed.

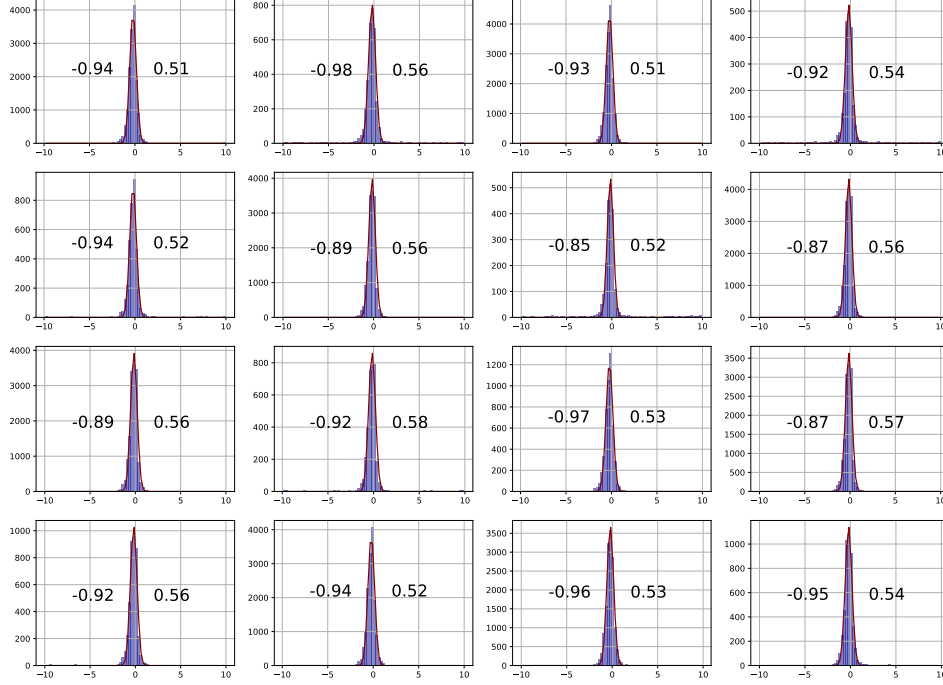


Figure 5: Gaussian fit of considered delays for each of the 16 measurement. The fit is done using SCIPY.OPTIMIZE.CURVE_FIT function. The 2 numbers in the boxes are the t_{min} and t_{max} for each file.

3 Coincidences count

In our data files we only have the channel detection at each instant, but we don't know whether the detected photons are entangled or not. We have to consider as entangled photons that arrives at the two different channel basically at the same time (considering some possible delay due to the experimental apparatus). The delay between each photon is calculated as following:

$$\Delta t = (t_i - t_{i-1}) \text{sign}(ch_i - ch_{i-1}) \quad (3.1)$$

Only the $\Delta t \neq 0$ are kept. In this way, we have a series of Δt negative and positive, distributed as a Gaussian function. Also, since only photons that arrives close can be considered as entangled, $\Delta t > 10$ ns and $\Delta t < -10$ ns are removed. What we get at the end is a Gaussian shape function, which can be fitted in order to consider all detection within 2σ and -2σ . This procedure is done for every file. In this case, the bounds chosen are $t_{min} = -0.97$ and $t_{max} = 0.58$, the upper and lower bounds. The procedure is show in Fig.5.

After this procedure, coincidences are counted as the number of delays within the interval defined above. In Tab.2 is shown a summary of the characteristics of each measurement.

4 CHSH parameter

Given the number of coincidences, it is possible to evaluate the CHSH parameters. The error associated with it is based on the Gaussian Error Propagation.

For each coincidence it is associated a Poissonian error $\delta N_{ii} = \sqrt{N_{ii}}$. The $E(\alpha, \beta)$ terms are made

Filename	α	β	Operator A	Operator B	Outcome A	Outcome B	Coincidences N_{ii}
x0a0y0b0	0°	-22.5°	A_1	B_1	+	+	13934
x0a0y0b1	0°	-22.5°	A_1	B_1	+	-	3180
x0a1y0b0	0°	-22.5°	A_1	B_1	-	+	3406
x0a1y0b1	0°	-22.5°	A_1	B_1	-	-	13826
x0a0y1b0	0°	22.5°	A_1	B_2	+	+	15372
x0a0y1b1	0°	22.5°	A_1	B_2	+	-	2048
x0a1y1b0	0°	22.5°	A_1	B_2	-	+	2023
x0a1y1b1	0°	22.5°	A_1	B_2	-	-	15033
x1a0y0b0	45°	-22.5°	A_2	B_1	+	+	13802
x1a0y0b1	45°	-22.5°	A_2	B_1	+	-	3329
x1a1y0b0	45°	-22.5°	A_2	B_1	-	+	3881
x1a1y0b1	45°	-22.5°	A_2	B_1	-	-	13718
x1a0y1b0	45°	22.5°	A_2	B_2	+	+	4505
x1a0y1b1	45°	22.5°	A_2	B_2	+	-	12620
x1a1y1b0	45°	22.5°	A_2	B_2	-	+	13322
x1a1y1b1	45°	22.5°	A_2	B_2	-	-	4288

Table 2: Summary of characteristics for each measurement. The first column is the filename, the second and third are the angles setting for A and B , the forth and fifth are the measurement operator for A and B , the sixth and seventh the output of the measurement, the last column are the number of coincidences detected.

up by a numerator and a denominator which have the same error, being it:

$$\delta e = \sqrt{(\delta N_{++})^2 + (\delta N_{+-})^2 + (\delta N_{-+})^2 + (\delta N_{--})^2} \quad (4.1)$$

At this point, the error associated with $E(\alpha, \beta)$ is:

$$\delta E(\alpha, \beta) = E(\alpha, \beta) \sqrt{\left(\frac{\delta e}{N_{++} + N_{--} - N_{+-} - N_{-+}}\right)^2 + \left(\frac{\delta e}{N_{++} + N_{--} + N_{+-} + N_{-+}}\right)^2} \quad (4.2)$$

And finally:

$$\delta S = \sqrt{(\delta E(\alpha, \beta))^2 + (\delta E(\alpha, \beta'))^2 + (\delta E(\alpha', \beta))^2 + (\delta E(\alpha', \beta'))^2} \quad (4.3)$$

According to Eq. 4.2, the results is:

$$S = 2.459 \pm 0.012 \quad (4.4)$$

Therefore the CHSH inequality is violated and the Bell's theorem is proven.